8 Supplementary Material

8.1 Introduction

Next to the previously reviewed alterations of target N200 and P300 with target congruency (see the Introduction section of the main paper), modulations of target P100 and N100 by the presence or absence of a foregoing cue have also been observed (Neuhaus et al. 2010; Williams et al. 2016). Such kind of alterations of target-locked early ERP components would be due to attentional top-down processes representing the amount of information used to direct visual attention. Target P100 amplitude was significantly higher at parietal sites in the no cue condition compared to the situation with a cue as well as when following a central cue compared to a spatial cue according to some authors (Williams et al. 2016), while other scientists observed a reversed orienting effect on target P100 amplitude in the parieto-occipital scalp regions (Galvao-Carmona et al. 2014). As a sign of amplified perceptual discrimination, alerting induced increased amplitude of target N100 over parietal leads (Neuhaus et al. 2010; Williams et al. 2016) whereas target N100 following orienting was enhanced over occipital and parieto-occipital leads (Neuhaus et al. 2010; Williams et al. 2016), though Galvao-Carmona et al. did not find any orienting effect for target N100 (Galvao-Carmona et al. 2014).

Concerning ERSPs associated with the standard ANT, according to Fan et al. (Fan et al. 2007), each attentional network may have a distinct set of oscillations related to its activity. In the context of the alerting and orienting networks, theta-, alpha- and beta-band activity has been shown to decrease at 200-450 ms after the presentation of a neutral cue and corresponds to the usual desynchronisation of electrical activity after a warning. Unlike Fan et al. (Fan et al. 2007), Deiber and colleagues (Deiber et al. 2013) observed a transient increase of theta power after the presentation of a cue. These oscillations known to be significantly phase-locked after the visualisation of a stimulus would contribute to the generation of P100 event-related component (Makeig et al. 2002; Klimesch et al. 2011). During the cue-target interval, ERDs in alpha and beta bands were observed (Deiber et al. 2013) and, as being proportional to the amount of information carried by the cue, these ERDs signal the level of attentional mobilisation prior to target occurrence (Klimesch 1999; Pfurtscheller 1999; Bastiaansen and Brunia 2001; Engel and Fries 2010; Tzagarakis et al. 2010). Concerning target-locked analysis, the executive control network (i.e. incongruent minus congruent target conditions) exhibited a complex time-frequency pattern: an early (<400 ms) increase of a broad-band activity including beta band, followed by a late (>400 ms) decrease of a broad-band activity including theta, alpha and beta bands (Fan et al. 2007). Indeed, Deiber et al. (Deiber et al. 2013) also found, together with a transient ERS in theta power, an ERD in alpha and beta bands after the target presentation, which was more pronounced for incongruent flankers. Furthermore, alerting and orienting effects on target-locked ERSPs have been observed (Fan et al. 2007). Firstly, under no cue and central cue conditions, an early ERS in some frequency components of beta band and

higher frequencies occurred between 100 and 300 ms after target presentation and was related to the orienting processing needed when the target surrounded by flankers appeared on the computer screen. In the case of a spatial cue preceding the target, such an ERS was therefore not seen. Second, a late target-locked ERD in theta-, alpha- and beta-band power was more pronounced under no cue condition compared to central cue and spatial cue conditions because this decrease in power was associated with the alerting status recruited for the target response (Fan et al. 2007).

On the strength of the above reported results for the standard seated ANT, the present section will present a secondary objective of the study: the replication of similar target-locked ERPs and ERSPs in the context of the ANT combined with step initiation.

8.2 Material and methods

8.2.1 Target-locked ERPs analysis

Target-locked ERPs were analysed with the EEGLAB toolbox (Delorme and Makeig 2004), with a baseline interval from 1500 to 1000 ms before target onset, in the context of comparison of target conditions. The time window analysis was from -200 ms before S2 to 1000 ms after. We first analysed ERP scalp distribution maps between 250 and 650 ms. Next, based on the observation of topographic maps of ERPs and according to the well-known topography of such ERP components (Berchicci et al. 2012), P300 wave's characteristics were assessed and collected by grand-averaging over the relevant midline electrode: Pz). P300 peak latencies and amplitudes of all the subjects were compared as a function of the conflict resolution condition (target surrounded by congruent vs. incongruent flankers). The amplitude of potentials was measured as the difference between the maximum peak of the ERP waveform and the mean baseline voltage. Latency was defined as the interval between target presentation and the point of peak amplitude in the time window of the potential. Time window of P300 ranged from 250 to 650 ms after target presentation. On the other hand, when we evaluated the alerting and orienting effects on target ERPs, we used a baseline interval from -200 ms until target presentation in order not to take into account the contingent negative variation which is not analysable because of the variable time interval between cue and target. The time window analysis was from -200 ms before S2 to 800 ms after, and ERP scalp distribution maps between 0 and 300 ms were observed in order to assess and collect N100 wave's features by grand-averaging over the relevant midline electrodes, i.e. Pz and POz (Di Russo et al. 2002, 2003). Finally, potential alerting and orienting effects on N100 peak latencies and amplitudes were evaluated. Time window associated with N100 ranged between 150 and 300 ms after S2. The grand-averaged ERPs were low-pass filtered at 40 Hz for displaying purpose only. It should be noted that N200 and P100 waves were not involved in the comparison between target and cue conditions, respectively, because these types of ERPs were not clearly visible in most individual event-related averages.

After the manual rejection of epochs of EEG data with artefacts, participants showed trials that were distributed as follows (median (first quartile - third quartile)): 125 (112.25 - 134.5) congruent trials, 116.5 (110.25 - 126.5) incongruent trials, and 40.5 (37 - 44.75), 48 (42.5 - 50), 115.5 (106.25 - 124), 39.5 (35.25 - 42) trials corresponding respectively to no cue condition, central cue condition, and both valid and invalid spatial cue conditions.

8.2.2 Target-locked ERSPs analysis

Target-locked ERSP data were also analysed using the EEGLAB toolbox (Delorme and Makeig 2004) with a baseline interval of between 1500 and 1000 ms before target presentation. In order to characterise event-related EEG oscillations such as ERD and ERS in theta (4-7 Hz), alpha (8-12 Hz) and beta (13-30 Hz) bands, we applied a time-frequency analysis using a continuous Morlet wavelet transform, with 2 cycles at the lowest frequency and 7.5 at highest (factor: 0.5), and analysed ERSP scalp distribution maps between 0 and 700 ms after S2.

8.2.3 MRCP source localisation

In order to have a more accurate idea of generators of MRCP, source localisation was performed on response-locked EEG data. To this end, MRI (template) and EEG data were co-registered via identification of the same anatomic landmarks (the left and right pre-auricular points and nasion). A realistic head model was built by segmenting the MRI data with Freesurfer software (Dale et al. 1999). The lead field matrix was then computed for a cortical mesh with 15000 vertices using Brainstorm software (Tadel et al. 2011) and OpenMEEG software (Gramfort et al. 2010). Afterwards, the weighted minimum norm estimate was used to reconstruct the dynamics of the EEG signal's cortical sources, using Brainstorm software. The obtained source matrices were finally averaged over epochs and subjects for each condition of cue and target in order to reflect sources of ERPs, and then averaged in time over a 200-ms time interval before APA onset.

8.2.4 Statistical analyses

By means of EEGLAB toolbox, permutation tests for multiple comparisons were performed on overall ERP and ERSP data with FDR correction. Afterwards, conflict resolution, alerting and orienting effects on specific ERP waveforms at particular scalp sites were assessed by using a Student's t-test or a Wilcoxon's signed rank test (if normality is not observed) on peak amplitude and latency, with SPSS 16.0 software. The threshold for statistical significance was set to $p=0.05$.

8.3 Results

8.3.1 Target-locked ERPs

In Fig. 7, a negative wave (corresponding to target N100) was seen on parietal and occipito-parietal leads. No significant orienting effect was associated with this ERP waveform, but an alerting effect on target N100 wave was observed at Pz and POz (Fig. 8), with a higher N100 amplitude in central cue condition compared to trials without a cue (respectively -2.28 ± 1.81 μV vs. -2.61 ± 2.08 μV at Pz with p=0.005, and -2.71 ± 1.87 μV vs. -3.08 ± 2.25 μV at POz with p=0.014).

Besides, the ERP scalp distribution maps between 250 and 650 ms revealed a positive component (corresponding to P300) in the step initiation task (see Fig. 9). Maximum amplitude was measured at Pz for both flanker conditions. The peak latency was significantly longer (p=0.002) in trials with incongruent flankers than in trials with congruent flankers, whereas the peak amplitude was not significantly different between target conditions (respectively 457 ± 108 ms vs. 426 ± 96 ms for peak latency, and 2.66 ± 2.36 μV vs. 2.88 ± 2.7 μV for peak amplitude).

8.3.2 Target-locked ERSPs

Regarding the effect of cues on target-related ERSPs, we noticed an alerting effect but no effect of orientation (see Fig. 10). Indeed, alpha and beta desynchronisations are related to attentional load and particularly warning and, over the somatosensory cortex and the motor cortex, they mirror the preparation phase toward the movement and the movement itself. These ERDs started significantly later in trials without cue compared to trials preceded by a central cue.

As shown in Fig. 11, time-frequency analysis of the alpha band revealed posterior ERD that tended to be more pronounced and lasted significantly longer in trials with incongruent flankers. The posterior suppression of alpha-band oscillatory activity was accompanied by anterior and central enhancements of alpha activity. Time-frequency analysis of the beta band revealed a central-posterior ERD that was also more pronounced and lasted significantly longer for incongruent flankers than for congruent flankers.

8.3.3 Localisation of MRCP sources

It was surprising to have observed a maximal BP at parietal leads while this motor potential is supposed to be symmetrically distributed and maximal at the midline centro-parietal area (Shibasaki and Hallett 2006). Thanks to MRCP source localisation averaged over a 200-ms time interval before APA onset (see Fig. 12), we confirmed the location of BP over the sensorimotor cortex, with the supplementary motor area as a potential generator. EEG activity was also found in orbito-frontal and temporal regions as a sign of attentional load.

8.4 Discussion regarding target-locked EEG activity

Target-locked ERPs: When mapping the ERPs between 250 and 650 ms after target presentation in a step initiation ANT, we observed a positive wave with a peak amplitude at Pz; this might correspond to the P300 component. An effect of conflict resolution on P300 amplitude was found. A lower P300 amplitude in the presence of incongruent flankers might be accounted for by the greater task difficulty in this condition (Polich 1987; Hagen et al. 2006) and might thus be associated with greater response inhibition (Groom and Cragg 2015). Contradictory results have also already been reported in ERP studies of the standard ANT, with a lower amplitude in incongruent trials in some studies (Neuhaus et al. 2007, 2010; Deiber et al. 2013; Galvao-Carmona et al. 2014) but not in others (Fan et al. 2007; Williams et al. 2016), and with a possible effect of age (Deiber et al. 2013). Furthermore, our analyses revealed target-related latency modulation. Indeed, in ANT combined with step initiation, the P300 peak latency was significantly longer in incongruent trials than in congruent trials. No previous studies of the standard ANT paradigm have reported target-related variations in latency (Fan et al. 2007; Neuhaus et al. 2010; Deiber et al. 2013; Galvao-Carmona et al. 2014) with the exception of Williams et al. and Neuhaus et al. (Neuhaus et al. 2007; Williams et al. 2016), who demonstrated that P300 peak latency was longer for incongruent flankers. The increased latency of P300 wave may mirror the use of more time to evaluate the target surrounded by incongruent flankers (Falkenstein et al. 1994; Verleger et al. 2006). Concerning the influence of cues on target-locked ERPs, we noticed an alerting effect on amplitude target N100, with higher target N100 amplitude over parietal and occipito-parietal electrodes for trials with a central cue compared to situations without any cue. It confirms what Neuhaus et al., Williams et al. and Galvao-Carmona and colleagues found (Neuhaus et al. 2010; Galvao-Carmona et al. 2014; Williams et al. 2016), although no orienting effect on target N100 amplitude was observed in this study unlike (Neuhaus et al. 2010; Williams et al. 2016). This increased target N100 amplitude related to alertness can be interpreted as an amplified perceptual discrimination of the target (Neuhaus et al. 2010) or an enhanced attention to the target (Williams et al. 2016), as N100 enhancement would mirror orienting to and enhanced processing of any input found relevant in a preliminary sensory analysis (Näätänen and Michie 1979).

Target-locked ERSPs: With regard to the ERSP data, we observed posterior alpha-band ERD and an anterior enhancement of alpha activity. This association has previously been described (Pfurtscheller 1999; Bastiaansen and Brunia 2001); alpha oscillatory activity was suppressed in areas engaged in visual attention, and ERS appeared concomitantly in brain regions not involved in stimulus processing or maintenance (Foxe and Snyder 2011; Deiber et al. 2013). In fact, ERS is thought to reflect the active inhibition of cortical regions, whereas ERD is thought to reflect the activation of regions engaged in visuospatial attention or motor execution (Pfurtscheller 1999). As reported in studies investigating the standard seated ANT and carried out by Deiber et al. (Deiber et al. 2013) and Fan et al. (Fan et al. 2007), alpha-band ERD tended to be more pronounced as well as of longer duration in trials with incongruent

flankers than in trials with congruent flankers - reflecting the greater attentional load. Concerning beta-band oscillations, our results showed central ERD that was more pronounced and lasted longer for incongruent trials than congruent trials in the step initiation ANT (as also reported by Deiber et al. (Deiber et al. 2013)). This reflects the specific participation of areas involved in motor preparation and execution. It is noteworthy that posterior alpha ERD and posterior and central beta ERD occurred around 200 ms after target presentation; this corresponds to movement preparation (the medians - for each subject - of the reaction time in our step initiation ANT ranged from 158 to 269 ms) but is also seen in attentional tasks (Klimesch et al. 2007). The influence of cues on target-locked ERSPs was rarely studied before. We found alpha and beta ERDs over the parietal cortex that started significantly later in trials without cue compared to trials preceded by a central cue, reflecting the increased perceptual discrimination of the target associated with the presence of a cue that was already shown through target-locked ERPs.

8.5 Figures

Fig. 7 Influence of cue modality on target-locked ERPs. a) ERP scalp distribution maps between 0 and 300 ms after presentation of the target, for trials with a central cue (first column), an invalid spatial cue (second column), a valid spatial cue (third column) and without cue (fourth column) in the step initiation ANT. Column to the right of ERP scalp distribution maps: significant differences in a permutation test with FDR correction (threshold at $p<0.05$) are marked as red dots. b) ERPs at Pz for the four kinds of cues. A negative wave (corresponding to N100) was observable. At the bottom, time intervals highlighted in black represent those for which the p-value related to permutation statistics with FDR correction is significant (i.e. < 0.05). CC = trials with a central cue; IO = trials with an invalid spatial cue; VO = trials with a valid spatial cue; NC = trials without cue

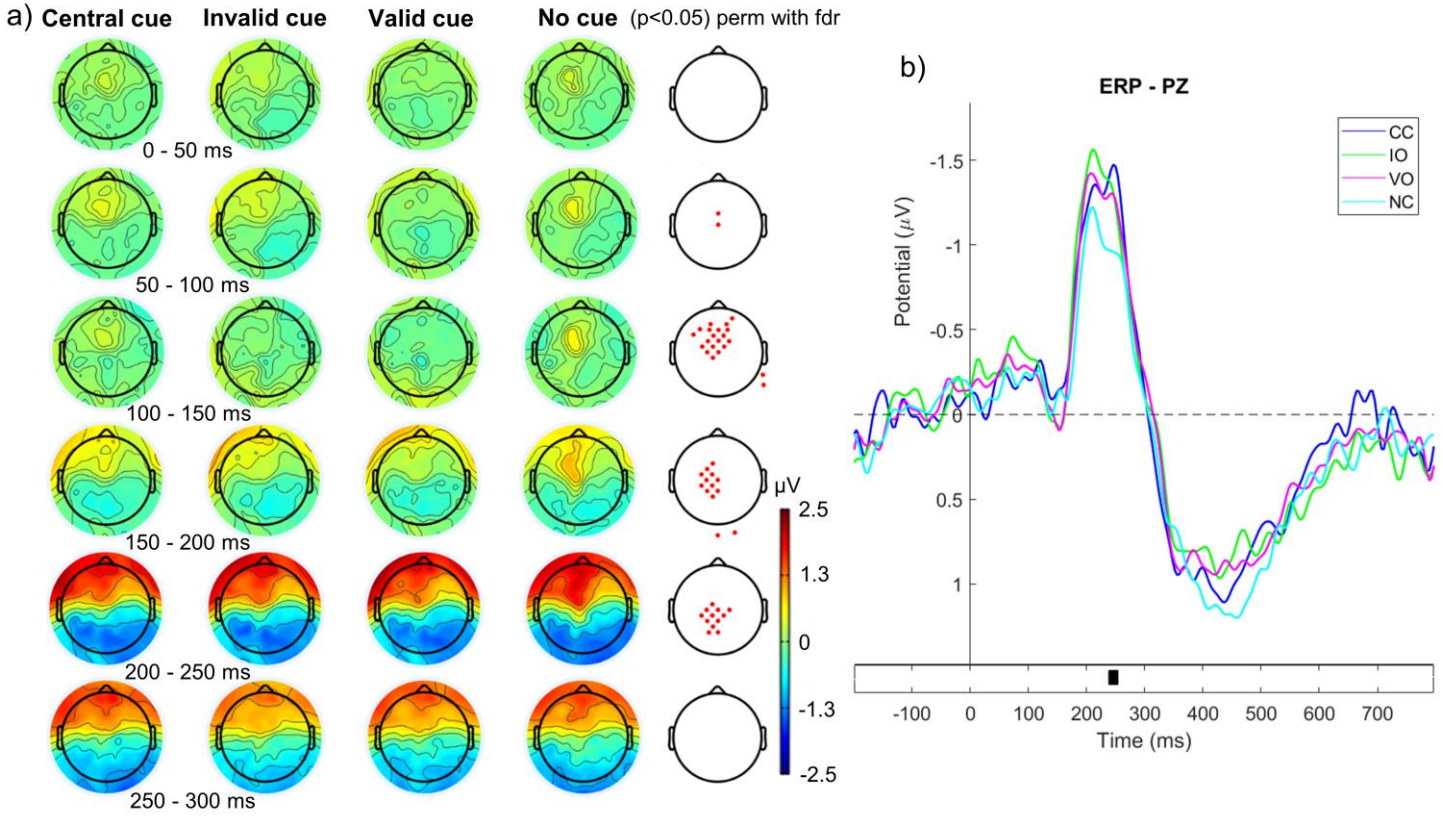

Fig. 8 Alerting effect on N100. a) ERP scalp distribution maps between 150 and 300 ms after presentation of the target, for trials with a central cue (CC, first column) and without cue (NC, fourth column) in the step initiation ANT. Column to the right of ERP scalp distribution maps: significant differences in a permutation test with FDR correction (threshold at $p<0.05$) are marked as red dots. b) ERPs at Pz and POz for trials with a central cue and without cue. A negative wave (corresponding to N100) was observable. At the bottom, time intervals highlighted in black represent those for which the p-value related to permutation statistics with FDR correction is significant (i.e. < 0.05). CC = trials with a central cue; NC = trials without cue

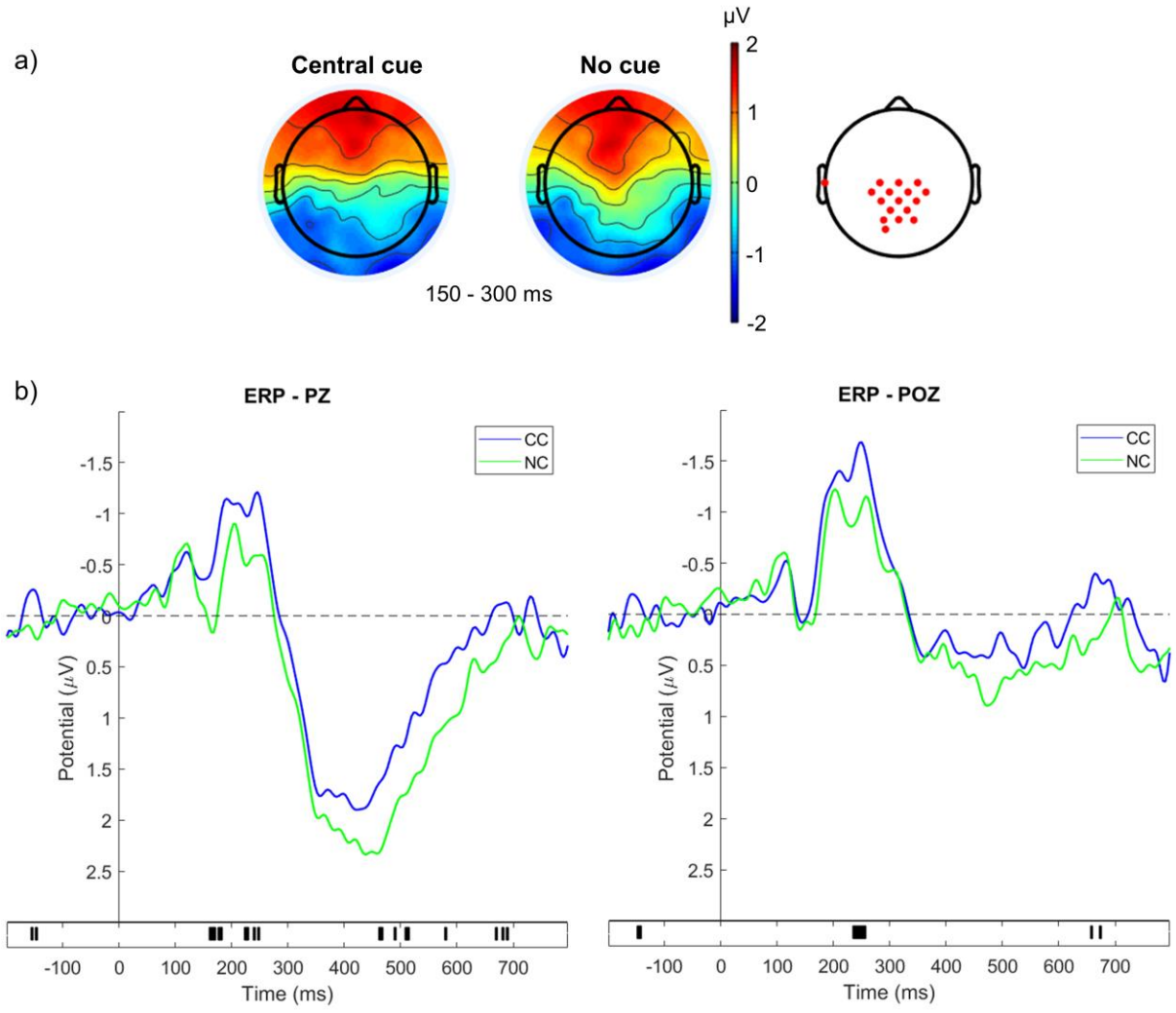

Fig. 9 Influence of target modality on ERPs. a) ERP scalp distribution maps between 250 and 650 ms after presentation of the target, for trials with congruent flankers (first column) or incongruent flankers (second column) in the step initiation ANT. Column to the right of ERP scalp distribution maps: significant differences in a permutation test with FDR correction (threshold at $p<0.05$) are marked as red dots. b) ERPs at Pz. A positive wave (corresponding to P300) was observable. At the bottom, time intervals highlighted in black represent those for which the p-value related to permutation statistics with FDR correction is significant (i.e. < 0.05). C = trials with congruent flankers; I = trials with incongruent flankers

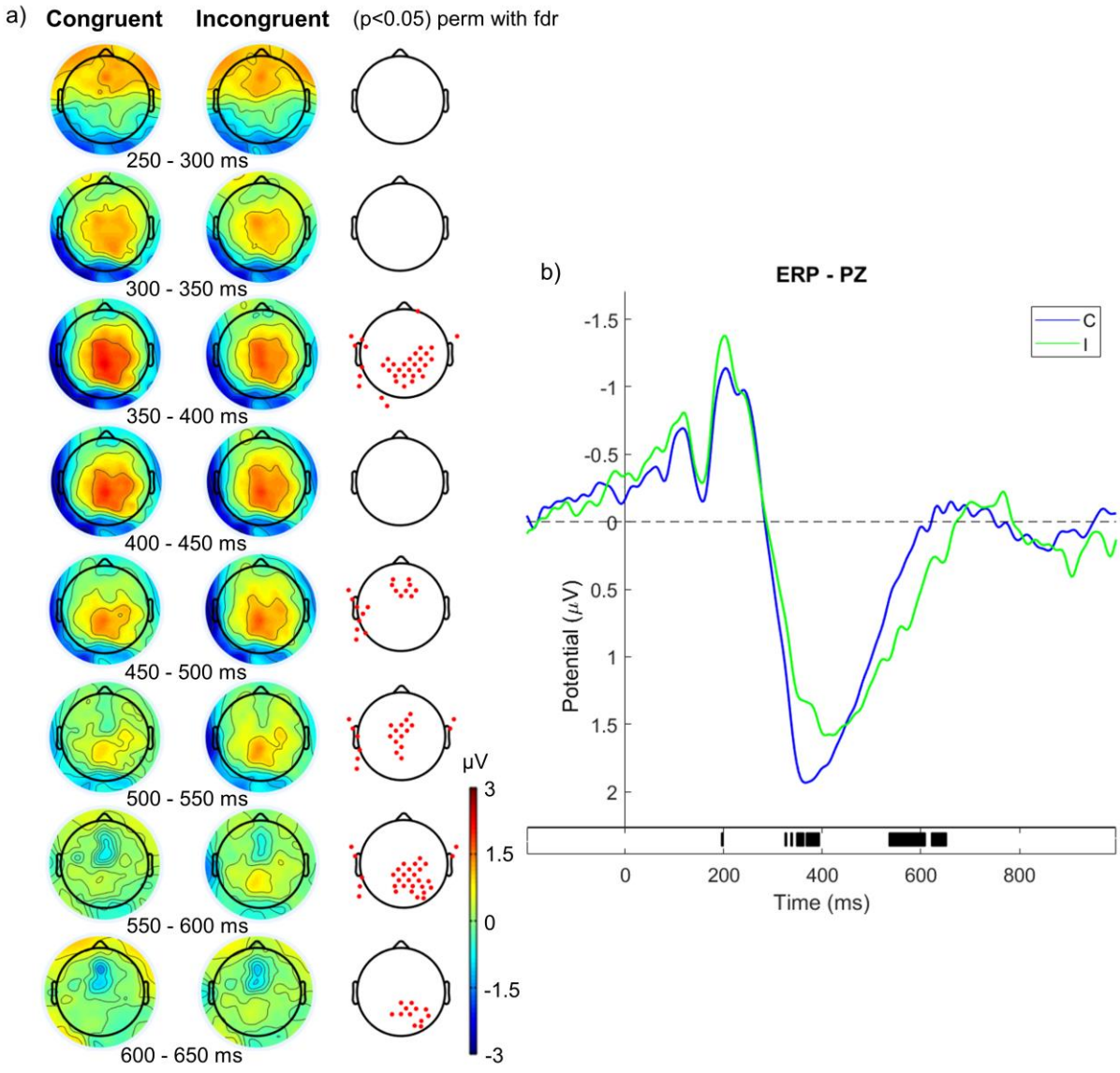

Fig. 10 Influence of cue modality on target-locked ERSPs. Target-locked topographic distributions of time-frequency energy (left: in alpha band (8-12 Hz); right: in beta band (13-30 Hz)), corresponding to the four cue conditions (central cue, invalid spatial cue, valid spatial cue and no cue) in the step initiation ANT. Time interval: between 0 and 700 ms after the presentation of the target. ERD is shown in blue and ERS is shown in red. Column to the right of spectral distributions in each frequency band: significant differences in a permutation test with FDR correction (threshold at $p<0.05$) are marked as red dots

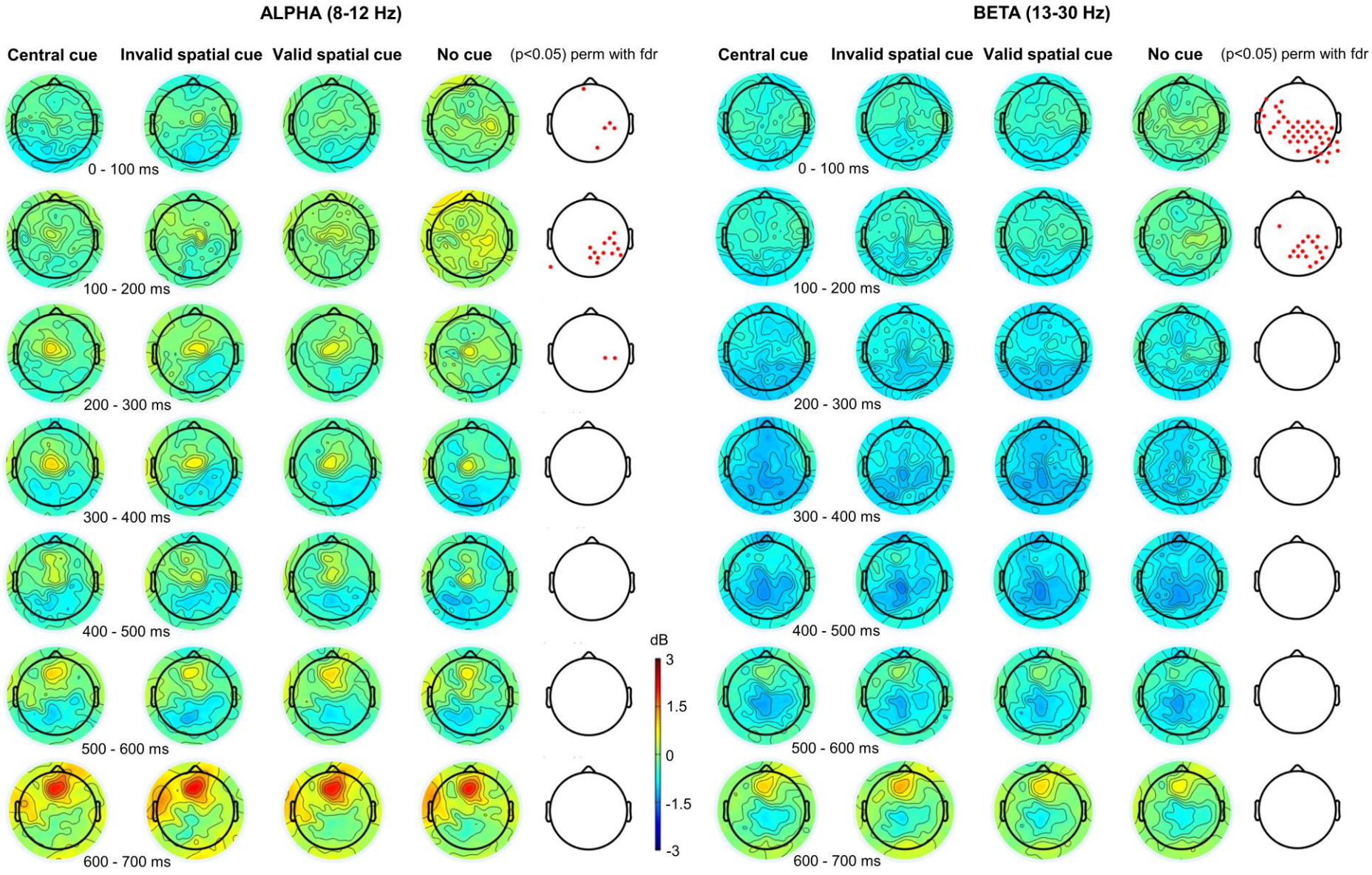
ALPHA (8-12 Hz)
BETA (13-30 Hz)
Central cue
Invalid spatial cue
Valid spatial cue
No cue
(p<0.05) perm with fdr
0 - 100 ms
100 - 200 ms
200 - 300 ms
300 - 400 ms
400 - 500 ms
500 - 600 ms
600 - 700 ms
dB
3
1.5
0
-1.5
-3

Fig. 11 Influence of target modality on target-locked ERSPs. Target-locked topographic distributions of time-frequency energy (left: in alpha band (8-12 Hz); right: in beta band (13-30 Hz)), corresponding to the two flanker conditions (congruent or incongruent) in the step initiation ANT. Time interval: between 0 and 700 ms after the presentation of the target. ERD is shown in blue and ERS is shown in red. Column to the right of spectral distributions in each frequency band: significant differences in a permutation test with FDR correction (threshold at $p<0.05$) are marked as red dots

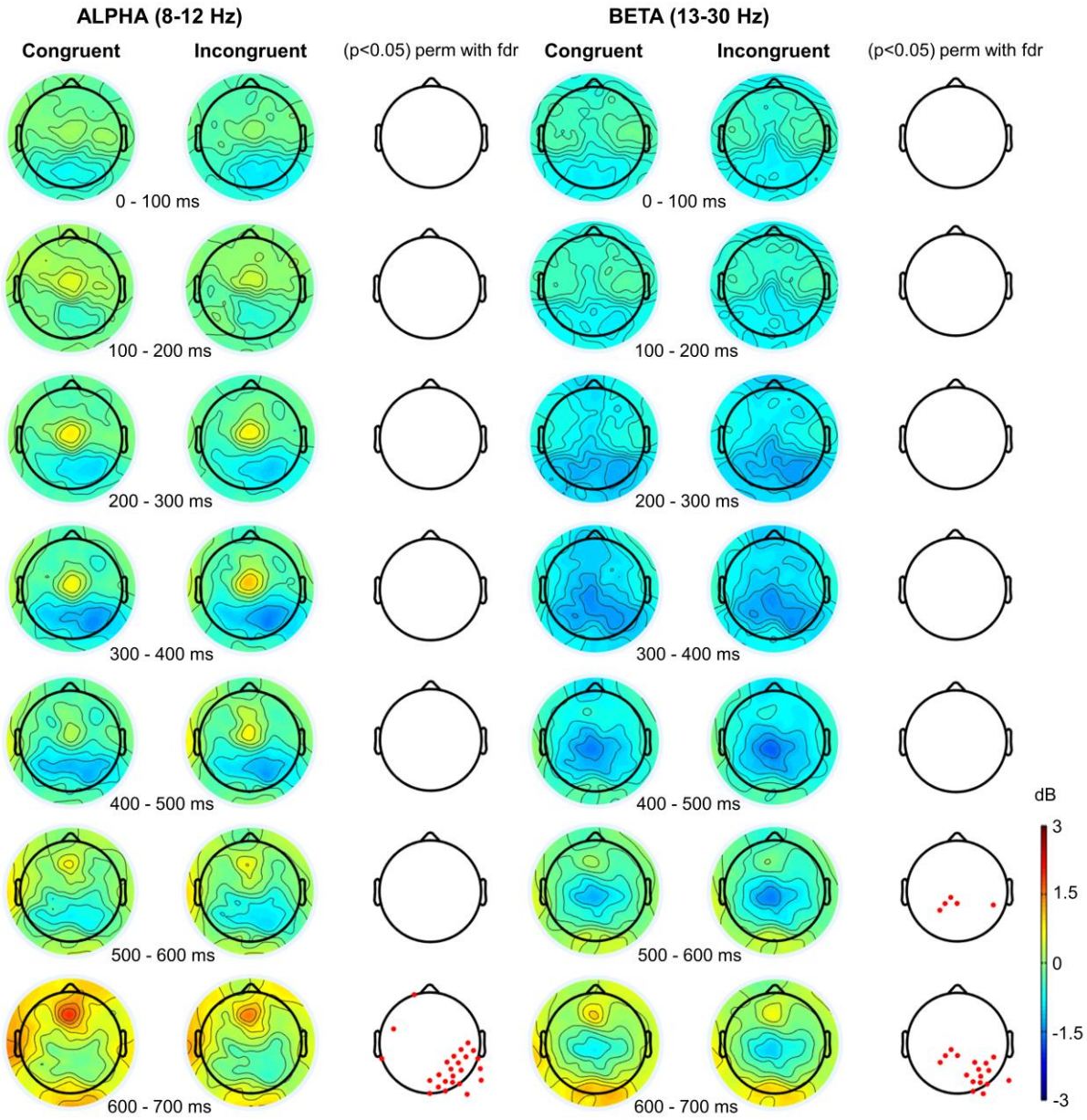

Fig. 12 Localisation of MRCP sources. a) Comparison of MRCP source localisation between conditions of cue during a time interval ranging from 200 ms before APA onset to the start of APA. b) Comparison of MRCP source localisation between conditions of target during a time interval ranging from 200 ms before APA onset to the start of APA

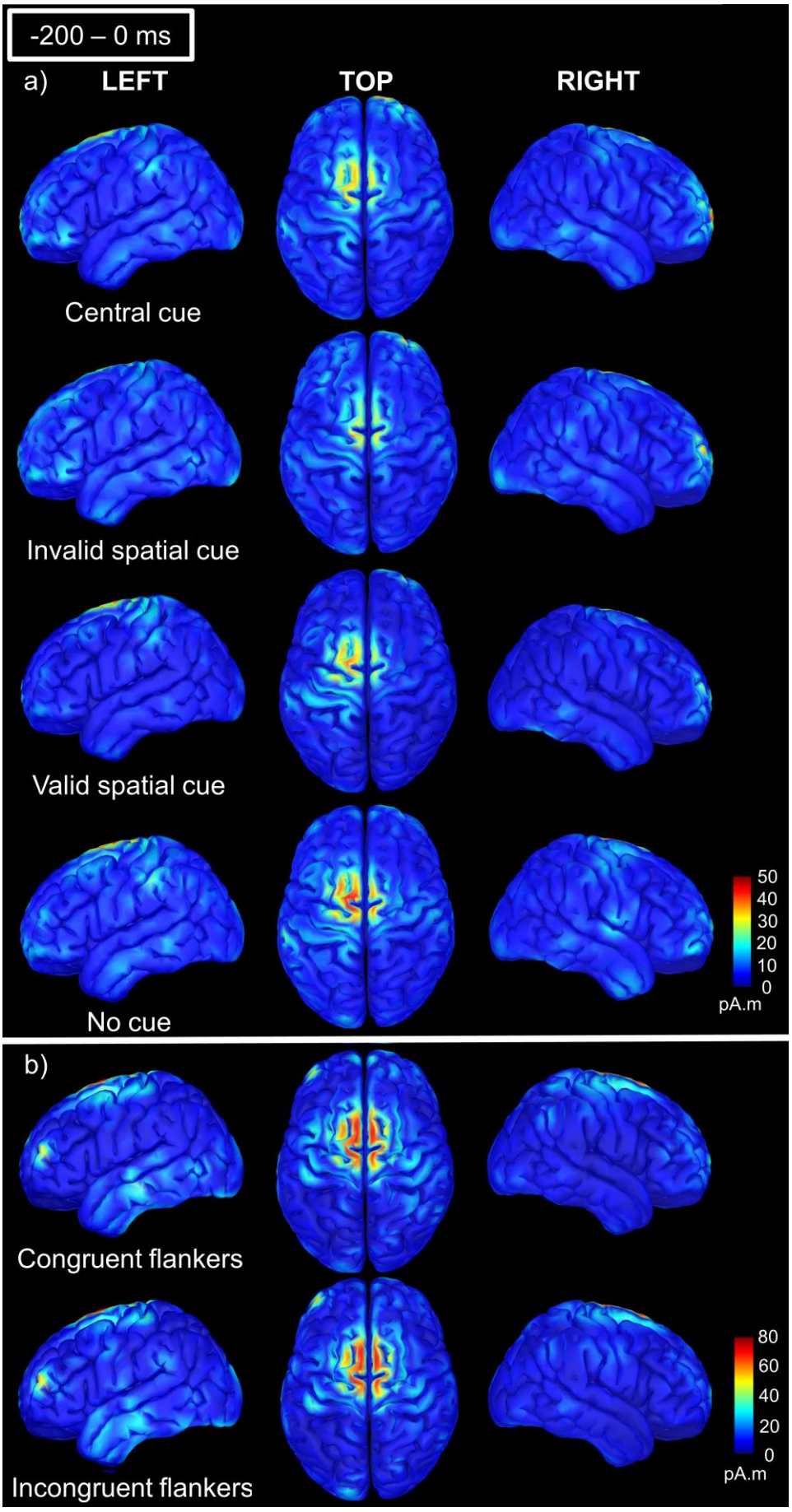
-200 – 0 ms
a)
LEFT
TOP
RIGHT
Central cue
Invalid spatial cue
Valid spatial cue
No cue
50
40
30
20
10
0
pA.m
b)
Congruent flankers
Incongruent flankers
80
60
40
20
0
pA.m

8.6 References

Bastiaansen MCM, Brunia CHM (2001) Anticipatory attention: an event-related desynchronization approach. Int J Psychophysiol 43:91–107. https://doi.org/10.1016/S0167-8760(01)00181-7

Berchicci M, Lucci G, Pesce C, et al (2012) Prefrontal hyperactivity in older people during motor planning. NeuroImage 62:1750–1760. https://doi.org/10.1016/j.neuroimage.2012.06.031

Dale AM, Fischl B, Sereno MI (1999) Cortical surface-based analysis. I. Segmentation and surface reconstruction. NeuroImage 9:179–194. https://doi.org/10.1006/nimg.1998.0395

Deiber M-P, Ibañez V, Missonnier P, et al (2013) Age-associated modulations of cerebral oscillatory patterns related to attention control. NeuroImage 82:531–546. https://doi.org/10.1016/j.neuroimage.2013.06.037

Delorme A, Makeig S (2004) EEGLAB: an open source toolbox for analysis of single-trial EEG dynamics including independent component analysis. J Neurosci Methods 134:9–21. https://doi.org/10.1016/j.jneumeth.2003.10.009

Di Russo F, Martínez A, Hillyard SA (2003) Source analysis of event-related cortical activity during visuo-spatial attention. Cereb Cortex N Y N 1991 13:486–499. https://doi.org/10.1093/cercor/13.5.486

Di Russo F, Martínez A, Sereno MI, et al (2002) Cortical sources of the early components of the visual evoked potential. Hum Brain Mapp 15:95–111

Engel AK, Fries P (2010) Beta-band oscillations--signalling the status quo? Curr Opin Neurobiol 20:156–165. https://doi.org/10.1016/j.conb.2010.02.015

Falkenstein M, Hohnsbein J, Hoormann J (1994) Effects of choice complexity on different subcomponents of the late positive complex of the event-related potential. Electroencephalogr Clin Neurophysiol 92:148–160

Fan J, Byrne J, Worden MS, et al (2007) The relation of brain oscillations to attentional networks. J Neurosci Off J Soc Neurosci 27:6197–6206. https://doi.org/10.1523/JNEUROSCI.1833-07.2007

Foxe JJ, Snyder AC (2011) The Role of Alpha-Band Brain Oscillations as a Sensory Suppression Mechanism during Selective Attention. Front Psychol 2:154. https://doi.org/10.3389/fpsyg.2011.00154

Galvao-Carmona A, González-Rosa JJ, Hidalgo-Muñoz AR, et al (2014) Disentangling the attention network test: behavioral, event related potentials, and neural source analyses. Front Hum Neurosci 8:813. https://doi.org/10.3389/fnhum.2014.00813

Gramfort A, Papadopoulo T, Olivi E, Clerc M (2010) OpenMEEG: opensource software for quasistatic bioelectromagnetics. Biomed Eng Online 9:45. https://doi.org/10.1186/1475-925X-9-45

Groom MJ, Cragg L (2015) Differential modulation of the N2 and P3 event-related potentials by response conflict and inhibition. Brain Cogn 97:1–9. https://doi.org/10.1016/j.bandc.2015.04.004

Hagen GF, Gatherwright JR, Lopez BA, Polich J (2006) P3a from visual stimuli: task difficulty effects. Int J Psychophysiol Off J Int Organ Psychophysiol 59:8–14. https://doi.org/10.1016/j.ijpsycho.2005.08.003

Klimesch W (1999) EEG alpha and theta oscillations reflect cognitive and memory performance: a review and analysis. Brain Res Rev 29:169–195. https://doi.org/10.1016/S0165-0173(98)00056-3

Klimesch W, Fellinger R, Freunberger R (2011) Alpha Oscillations and Early Stages of Visual Encoding. Front Psychol 2:. https://doi.org/10.3389/fpsyg.2011.00118

Klimesch W, Sauseng P, Hanslmayr S (2007) EEG alpha oscillations: the inhibition-timing hypothesis. Brain Res Rev 53:63–88. https://doi.org/10.1016/j.brainresrev.2006.06.003

Makeig S, Westerfield M, Jung T-P, et al (2002) Dynamic Brain Sources of Visual Evoked Responses. Science 295:690–694. https://doi.org/10.1126/science.1066168

Näätänen R, Michie PT (1979) Early selective-attention effects on the evoked potential: a critical review and reinterpretation. Biol Psychol 8:81–136

Neuhaus AH, Koehler S, Opgen-Rhein C, et al (2007) Selective anterior cingulate cortex deficit during conflict solution in schizophrenia: an event-related potential study. J Psychiatr Res 41:635–644. https://doi.org/10.1016/j.jpsychires.2006.06.012

Neuhaus AH, Urbanek C, Opgen-Rhein C, et al (2010) Event-related potentials associated with Attention Network Test. Int J Psychophysiol Off J Int Organ Psychophysiol 76:72–79. https://doi.org/10.1016/j.ijpsycho.2010.02.005

Pfurtscheller G (1999) Event-related EEG/MEG synchronization and desynchronization: basic principles. Clin Neurophysiol Off J Int Fed Clin Neurophysiol 110:1842–1857

Polich J (1987) Task difficulty, probability, and inter-stimulus interval as determinants of P300 from auditory stimuli. Electroencephalogr Clin Neurophysiol 68:311–320

Shibasaki H, Hallett M (2006) What is the Bereitschaftspotential? Clin Neurophysiol Off J Int Fed Clin Neurophysiol 117:2341–2356. https://doi.org/10.1016/j.clinph.2006.04.025

Tadel F, Baillet S, Mosher JC, et al (2011) Brainstorm: A user-friendly application for MEG/EEG analysis. Comput Intell Neurosci 2011:. https://doi.org/10.1155/2011/879716

Tzagarakis C, Ince NF, Leuthold AC, Pellizzer G (2010) Beta-Band Activity during Motor Planning Reflects Response Uncertainty. J Neurosci 30:11270–11277. https://doi.org/10.1523/JNEUROSCI.6026-09.2010

Verleger R, Jaśkowski P, Wascher E (2006) Evidence for an Integrative Role of P3b in Linking Reaction to Perception. J Psychophysiol

Williams RS, Biel AL, Wegier P, et al (2016) Age differences in the Attention Network Test: Evidence from behavior and event-related potentials. Brain Cogn 102:65–79. https://doi.org/10.1016/j.bandc.2015.12.007